VIP Photopolymerization Very Important Paper

International Edition: DOI: 10.1002/anie.201510037
German Edition: DOI: 10.1002/ange.201510037

Light-Regulated Polymerization under Near-Infrared/Far-Red Irradiation Catalyzed by Bacteriochlorophyll *a*

*Sivaprakash Shanmugam, Jiangtao Xu, and Cyrille Boyer**

Abstract: *Photoregulated polymerizations are typically conducted using high-energy (UV and blue) light, which may lead to undesired side reactions. Furthermore, as the penetration of visible light is rather limited, the range of applications with such wavelengths is likewise limited. We herein report the first living radical polymerization that can be activated and deactivated by irradiation with near-infrared (NIR) and far-red light. Bacteriochlorophyll a (Bachl a) was employed as a photoredox catalyst for photoinduced electron transfer/reversible addition–fragmentation chain transfer (PET-RAFT) polymerization. Well-defined polymers were thus synthesized within a few hours under NIR ($\lambda = 850$ nm) and far-red ($\lambda = 780$ nm) irradiation with excellent control over the molecular weight ($M_n/M_w < 1.25$). Taking advantage of the good penetration of NIR light, we showed that the polymerization also proceeded smoothly when a translucent barrier was placed between light source and reaction vessel.*

One of the central events that led to the development of life on earth was the advent of oxygen-evolving photosynthesis.[1] Oxygenic photosynthesis uses chlorophylls and visible light (blue to red wavelengths) to oxidize water to molecular oxygen and to produce carbohydrates, which sustain life. Until 1977, it was the only known mechanism capable of sustaining life. The discovery of phototrophic bacteria in hydrothermal vents resulted in a total change in this notion. These bacteria utilize another type of photosynthesis, which does not produce oxygen, and uses sulfide, elemental sulfur, or hydrogen instead of water as an electron donor. Hydrothermal vents, such as black smokers, are inhabited by such phototrophic bacteria that thrive in sun-starved conditions by carrying out anoxygenic (bacteriochlorophyll) photosynthesis.[2] Photosynthetic life in dark deep-sea vents resembles the environment in which life evolved, with the survival of these organisms relying on their ability to harvest geothermal light emitted by erupting superheated waters.[2a,3]

This form of photosynthesis (anoxygenic photosynthesis) utilizes light in the longer visible and near-infrared range, with the wavelength specificity being highly dependent on the type of bacterium. Bacteriochlorophylls (bacteriochlorophyll *b*) present in purple bacteria absorb at 900 or >1000 nm, whereas other bacteriochlorophylls absorb around 750 and 800 nm.[3] The photosynthetic potential in these ecosystems is rather low for most species. Bacteria possessing light-harvesting bacteriochlorophyll (BChl) that absorbs in the near-infrared region are able to harvest meager portions of the geothermal light generated by hydrothermal vents to oxidize sulfur compounds (H_2S and others) to reduce carbon dioxide to organic carbon.[2a,4]

Taking a step back and looking at the evolution of photosynthesis provides a novel avenue for polymer science that has remained unexplored thus far, especially for controlled/living radical polymerization (CLRP).[5] Current progress in CLRP has been centered on using visible light as an external regulator to initiate photopolymerization.[6] Most of these polymerization techniques use high-energy wavelengths (i.e., UV light ($\lambda \approx 350$ nm) and blue light ($\lambda \approx 460$ nm)) that could result in unwanted side reactions.[7] As a result, very limited attempts[8] have been made in expanding current work on visible-light polymerization to include more wavelengths of the solar spectrum, especially the near-infrared (NIR) region. Although visible-light-activated/deactivated polymerization provides numerous advantages in terms of spatial and temporal control,[9] it suffers from a lack of penetration depth. Herein, we present the first example of a green approach for NIR light mediated CLRP by using bacteriochlorophyll *a* (BChl *a*) as a biocatalyst to initiate the polymerization.[10] We successfully implemented, for the first time, the use of BChl *a* to mediate a photoinduced electron transfer/reversible addition–fragmentation chain transfer (PET-RAFT) polymerization.[11] Furthermore, we took advantage of the deep penetration of NIR light by performing the first CLRP in a vessel screened by a standard A4 white paper barrier as a model study.

BChl *a* plays a critical role during the initial stages of bacterial photosynthesis as a pigment for light harvesting, energy migration, and electron transport reactions.[12] Unlike chlorophylls found in plants, bacteriochlorophylls have absorption spectra that are principally centered in the near-infrared region of the light spectrum.[3] Drawing inspiration from NIR-based photosynthesis, we attempted to mimic nature by synthesizing advanced polymers with a NIR light source and BChl *a* through our established PET-RAFT process. BChl *a* displays remarkable photophysical properties owing to a high intersystem crossing rate (k_{ISC}) with low fluorescence (k_F) and internal conversion rates (k_{IC}; see the Supporting Information, Table S1)[13] and a low reduction potential (ca. −1.1 V vs. SCE),[14] which deems this molecule an ideal photoredox catalyst. Furthermore, the high quantum yield of intersystem crossing from the singlet excited state (S_1)

[*] S. Shanmugam, Dr. J. Xu, Prof. Dr. C. Boyer
Centre for Advanced Macromolecular Design and Australian Centre for NanoMedicine, School of Chemical Engineering
The University of New South Wales
Sydney, NSW 2052 (Australia)
E-mail: cboyer@unsw.edu.au
Homepage: http://www.camd.unsw.edu.au/

Supporting information for this article is available on the WWW under http://dx.doi.org/10.1002/anie.201510037.

to the lowest triplet state (T_1), often referred to as the triplet yield, increases the probability for photoinduced electron transfer (PET) to take place from excited π-conjugated BChl *a* to RAFT agents. Moreover, control experiments have shown that only the activation of CPADB (cyanopentanoic acid dithiobenzoate) in the presence of BChl *a* (Table S2, entries 3 and 6) led to efficient polymerization of methyl methacrylate (MMA) in both the far-red and NIR regions. In the absence of CPADB, negligible monomer conversion (<5%) was observed owing to direct activation from BChl *a* (Table S2, entries 1 and 4) for both wavelengths for an irradiation period of 24 hours. More importantly, in the absence of BChl *a*, no polymerization was observed even after irradiation for 24 hours at both wavelengths (Table S2, entries 2 and 5), which demonstrates that the absence of polymerization is due to photolysis of the RAFT agent as well as monomer activation, as previously observed under blue-light irradiation, and potential monomer degradation.[15] Furthermore, the efficiency of BChl *a* in promoting polymerization was compared with that of a RAFT agent with a much higher reduction potential; the polymerization of methyl acrylate (MA) in the presence of 2-(*n*-butyltrithiocarbonate)propionic acid (BTPA; Table S2, entry 10) proceeded much more slowly than with other PET-RAFT systems. Whereas the reduction potentials of CPADB and BTPA are much higher than that of BChl *a,* CPADB has a much higher reduction potential than BTPA (−0.4 V vs. −0.6 V, respectively), which makes the former more susceptible to reduction.[11] The reduction of RAFT agents in the presence of BChl *a* can lead to the generation of radicals that participate in RAFT polymerization (Scheme 1).[16] The radicals can be deactivated by excited-state cationic bacteriochlorophyll *a*, BChl $a^{+\bullet}$, leading to the regeneration of ground-state BChl *a* and the RAFT agent, which can restart the cycle.

The absorption spectrum of BChl *a* (Figure 1, black line) shows strong absorption from the visible to the NIR region of the solar spectrum. One of the advantages of BChl *a* in PET-RAFT stems from the fact that a higher efficiency of polymerization can be achieved with wavelengths of lower energy, particularly with far-red and NIR light. This is due to reduced interference, which arises from the higher molar

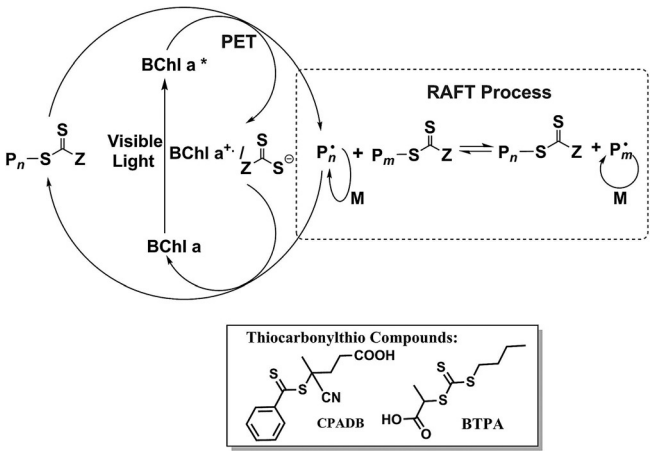

Scheme 1. Proposed mechanism for PET-RAFT polymerization using BChl *a* as the photocatalyst.

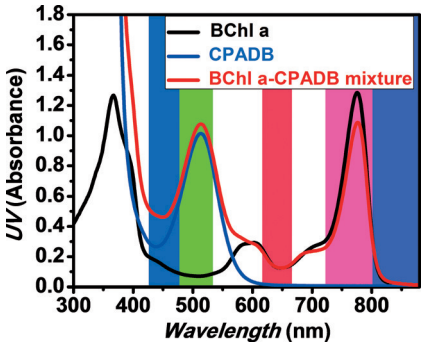

Figure 1. Overlay of the absorption wavelengths of CPADB, BChl *a*, and a mixture of BChl *a*/CPADB determined with LED lamps with different wavelength ranges. NIR (λ_{max} = 850 nm), far-red (λ_{max} = 780 nm), red (λ_{max} = 635 nm), green (λ_{max} = 530 nm), and blue (λ_{max} = 460 nm) LED light sources were employed in this study.

absorption coefficients in the far-red and NIR region than in other regions of the visible spectrum and the absence of an absorption overlap between the RAFT agent and BChl *a* (Table S3). Initial polymerizations of MMA and CPADB with BChl *a* were carried out under NIR (λ_{max} = 850 nm), far-red (λ_{max} = 780 nm), red (λ_{max} = 635 nm), green (λ_{max} = 530 nm), and blue (λ_{max} = 460 nm) LED irradiation. As BChl *a* has an intense absorption in the far-red region, the polymerization of MMA (Table S2, entry 6 and Table S3) was fastest at this wavelength with high monomer conversion (>70%), followed by polymerization in the NIR (Table S2, entry 3) and red region (Table S2, entry 7). It is interesting to note that polymerization under blue (Table S2, entry 9) and green (Table S2, entry 8) irradiation was quite slow, mainly owing to the low absorption of BChl *a* in these regions (Table S3) and also because of competitive absorption of CPADB and BChl *a* as shown in the overlay of the UV/Vis absorption spectra of BChl *a* and CPADB (Figure 1). Compared with BChl *a*, the molar absorption coefficient of CPADB is much lower in the blue and green region, with negligible absorption in the red, far-red, and NIR regions (Table S3). The competitive absorption in the blue and green regions may contribute to undesired quenching of the photoredox catalyst, resulting in its lower efficiency to promote polymerization at these wavelengths.[16d] The implementation of far-red and NIR absorbing biocatalysts such as BChl *a* in PET-RAFT can prevent this problem and ensure efficient polymerization.

As this is the first report on living radical polymerization under far-red and NIR irradiation, we investigated the polymerization kinetics by online Fourier transform near-infrared (FT-NIR) spectroscopy under far-red and near-infrared irradiation. We carried out the polymerization of MMA with different concentrations of BChl *a* (60 ppm and 15 ppm relative to the monomer concentration) to understand the effect of catalyst concentration on the kinetics of the polymerization for both light sources. As expected, the polymerization rate of MMA for both catalyst concentrations was faster under far-red than under NIR irradiation owing to the higher absorption of BChl *a* in the former region (Figure 1 A and Figure S3 A). At 15 ppm catalyst concentration (Figure 2 A), we observed a linear increase in $Ln([M]_0/[M]_t)$

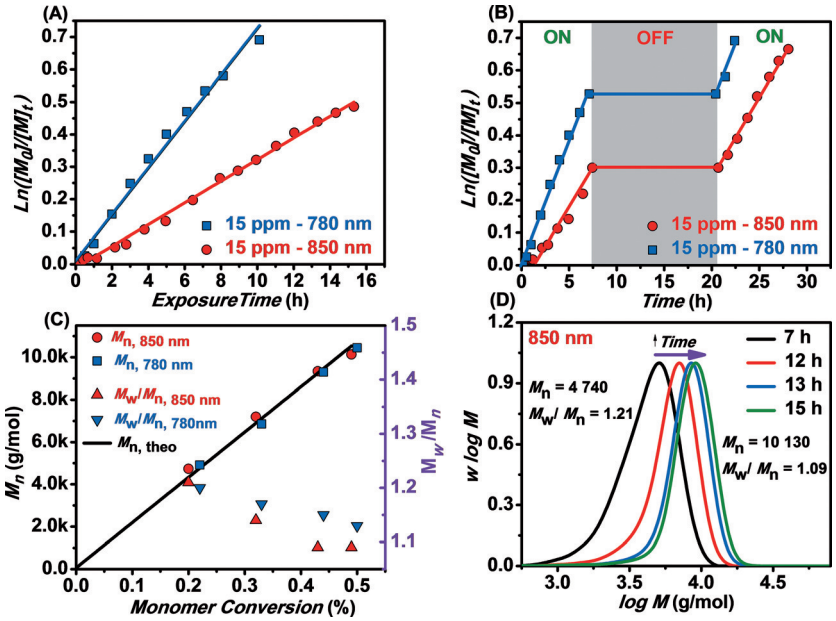

Figure 2. Online FT-NIR measurements to determine the kinetics of the PET-RAFT polymerization of MMA with BChl *a* as the photoredox biocatalyst and CPADB as the chain transfer agent under far-red ($\lambda_{max}=780$ nm, 104.9 mW cm^{-2}) and NIR ($\lambda_{max}=850$ nm, 40.00 mW cm^{-2}) irradiation, using a molar ratio of MMA/CPADB/BChl *a* = 209:1:3 × 10^{-3} in DMSO. A) Dependence of Ln ($[M]_0/[M]_t$) on exposure time under NIR (red circles) and far red (blue squares) irradiation. B) Dependence of Ln ($[M]_0/[M]_t$) on the exposure time under NIR (red circles) and far-red (blue squares) irradiation that was switched on and off. C) Dependence of M_n on the conversion under NIR and far-red irradiation. D) Molecular weight distributions after exposure to NIR irradiation for different periods of time.

with exposure time, suggesting a constant concentration of propagating radicals throughout the polymerization, with a higher propagation rate constant under far-red than under NIR irradiation ($k_p^{app}{}_{(far\text{-}red)} = 7.17\times10^{-2}$ h^{-1} vs. $k_p^{app}{}_{(NIR)} = 3.34\times10^{-2}$ h^{-1}). Furthermore, no inhibition period was observed in the far-red-mediated polymerization in contrast to a 45 min inhibition period for NIR polymerization, which can be related to the higher activation rate of CPADB by the photocatalyst under far-red irradiation. A similar trend was also observed at a catalyst concentration of 60 ppm, where a similar inhibition period ($t_{far\text{-}red,inh.} = 0$ h and $t_{NIR,inh.} =$ 45 min) and a higher concentration of propagating radicals were observed under far-red than under NIR irradiation (Figure S3 A; $k_p^{app}{}_{(far\text{-}red)} = 1.03\times10^{-1}$ h^{-1} vs. $k_p^{app}{}_{(NIR)} = 6.84\times10^{-2}$ h^{-1}).

Furthermore, we were able to reversibly activate and deactivate the polymerization process by switching the light source on and off. Upon irradiation with far-red and NIR light sources for catalyst concentrations of 15 and 60 ppm (Figure 2 B and Figure S3 B), the polymerization of MMA was activated whereas the absence of irradiation completely suppressed polymerization. Moreover, a plot of M_n and the polydispersity against monomer conversion revealed characteristics of a living radical polymerization: a linear increase in M_n, close agreement of the theoretical and experimental molecular weights, and a decrease in polydispersity with increasing monomer conversion (Figure 2 C and Figure S3 C). Finally, molecular weight distributions determined by gel-permeation chromatography (GPC) showed a symmetric shift from low to high molecular weights during the polymerization (Figure 2 D and Figures S3 D and S4).

High end-group fidelity (> 95 %) was observed by NMR spectroscopy for polymerization under both far-red and NIR irradiation (Figures S5 and S6). Furthermore, chain-extension experiments with MMA and *tert*-butyl methacrylate (*t*BuMA) were also carried out with the PMMA macroinitiator (Figures S7 and S8) to demonstrate the living character of this polymerization and the integrity of the end groups. The synthesis of the PMMA macroinitiator was performed under far-red and NIR illumination in DMSO at a catalyst concentration of 15 ppm ($M_{n,GPC} =$ 11 730 g mol^{-1}, $M_w/M_n = 1.11$, and 47 % monomer conversion for far-red and $M_{n,GPC} = 10\,700$ g mol^{-1}, $M_w/M_n = 1.10$, and 54 % monomer conversion for NIR irradiation). After purification of the macroinitiator through precipitation, successful chain extensions were investigated with MMA and *t*BuMA with a molar ratio of monomer/macroinitiator/BChl *a* of 500:1:7.5 × 10^{-3}. Under far-red irradiation (Figure S7), a complete shift in the molecular weight of the PMMA macroinitiator was observed, which was accompanied by the synthesis of diblock copolymers with narrow molecular weight distributions ($M_{n,GPC} = 17\,570$ g mol^{-1}, $M_w/M_n = 1.09$, and 12 % monomer conversion for PMMA-*b*-P*t*BuMA and $M_{n,GPC} = 15\,000$ g mol^{-1}, $M_w/M_n = 1.08$, and 7 % monomer conversion for PMMA-*b*-PMMA in 2 h). Under NIR irradiation (Figure S8), a similar complete shift in the molecular weight of the PMMA macroinitiators and the synthesis of diblock copolymers with narrow molecular weight distributions were observed ($M_{n,GPC} = 27\,950$ g mol^{-1}, $M_w/M_n = 1.08$, and 26 % monomer conversion for PMMA-*b*-P*t*BuMA and $M_{n,GPC} = 15\,500$ g mol^{-1}, $M_w/M_n = 1.08$, and 10 % monomer conversion for PMMA-*b*-PMMA in 12 h). To demonstrate the versatility of this polymerization and the robustness of the catalyst, various functional monomers, including glycidyl methacrylate (GMA), 2-dimethylaminoethyl methacrylate (DMAEMA), and oligo(ethylene glycol) methyl ether methacrylate (OEGMA, $M_n = 300$ g mol^{-1}), were investigated. All of these monomers were successfully polymerized with good control over the molecular weight and the molecular weight distributions ($M_w/M_n < 1.3$; Table S4).

One of the remarkable features of NIR light between 700 and 900 nm is its minimal absorption and scattering, which enables its use for a wide range of applications in medicine for both diagnosis and treatment.[17] Encouraged by these properties, we decided to exploit the penetration properties of such wavelengths by carrying out the polymerization in a vessel screened by a translucent barrier, namely a sheet of paper with a thickness of roughly 0.05 mm. Successful polymerization of MMA with NIR and far-red LED light sources

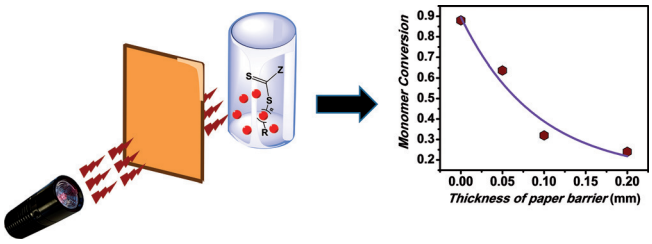

Scheme 2. PET-RAFT polymerization of MMA in the presence of a paper barrier (left) and the dependence of monomer conversion after NIR irradiation for 20 hours on the thickness of the paper (right).

screened by a single sheet of paper as a barrier (Scheme 2, left) was performed with BChl *a* as the photocatalyst for 20 hours. At a catalyst concentration of 60 ppm (Figure 3A), we observed a linear increase in $\mathrm{Ln}[\mathrm{M}]_0/[\mathrm{M}]_t$ with exposure time for both far-red and NIR polymerization, with both polymerizations having an inhibition period of up to 2 hours. Furthermore, the propagation rate constant for the polymerization with the NIR light source was greater than the apparent propagation rate constant for the far-red light source ($k_p^{app}{}_{(NIR)} = 5.21\times10^{-2}\ h^{-1}$ vs. $k_p^{app}{}_{(far\text{-}red)} = 3.16\times10^{-2}\ h^{-1}$). Surprisingly, in contrast to the polymerizations without the screen, the polymerization rate with a NIR source was faster than that with the far-red one despite the absorption of the photocatalyst being much lower under the former than under the latter conditions. These expected results can be attributed to the higher transmittance of NIR light compared to far-red light through the paper barrier. Indeed, in the presence of a paper screen, we observed a larger decrease in intensity for far-red light (from 104.9 to 19.74 mW cm^{-2}) than for NIR light (from 40.00 to 23.75 mW cm^{-2}). Furthermore, we were able to retain the reversible activation/deactivation of the near-infrared polymerization by switching the light source on and off even in the presence of a barrier (Figure 3B and Figure S9). A plot of M_n and the polydispersity against monomer conversion also revealed characteristics of a living radical polymerization, with close agreement between the theoretical and experimental molecular weights and a decrease in polydispersity with increasing monomer conversion (Figure 3C). Finally, a symmetric shift from low to high molecular weights was observed during the polymerization, as revealed by the molecular weight distributions determined by GPC (Figure 3D and Figure S10). As we were able to carry out the polymerization of MMA through a single sheet of paper (ca. 0.05 mm thick), we attempted to push the boundaries of NIR polymerization by increasing the thickness of the paper to 0.1 and 0.2 mm. As the intensity of the NIR light decreases with increasing paper thickness (23.75 mW cm^{-2} for 0.05 mm, 13.75 mW cm^{-2} for 0.1 mm, and 5.017 mW cm^{-2} for 0.2 mm), a drop in monomer conversion was observed for similar polymerization times (Scheme 2, left). Nevertheless, we were able to perform CLRP (Table S5) with good control over the molecular weights and the molecular weight distributions and theoretical molecular weights in good agreement with the experimental ones.

In summary, far-red and near-infrared light has been successfully employed for the activation of PET-RAFT polymerization with a biocatalyst (bacteriochlorophyll *a*). These polymerizations were extremely efficient as only a low light intensity was required to activate the polymerization. At the same time, the ability of near-infrared light to penetrate through a translucent barrier was utilized to perform the first CLRP in the presence of paper barriers with various thicknesses. This report suggests a range of potential biomedical and industrial applications for PET-RAFT polymerization, especially for applications requiring deep penetration.

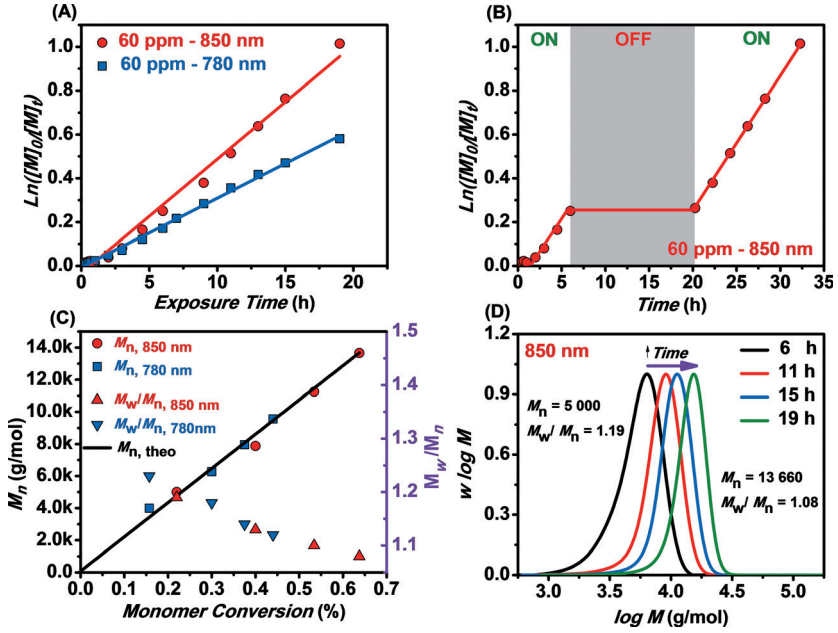

Figure 3. FT-NIR measurements to determine the kinetics of the PET-RAFT polymerization of MMA with BChl *a* and CPADB in the presence of a paper barrier under far-red (λ_{max} = 780 nm, 19.74 mW cm^{-2}) and NIR (λ_{max} = 850 nm, 23.75 mW cm^{-2}) irradiation, for a molar ratio of MMA/CPADB/BChl *a* = 209:1:1.2×10^{-2} in DMSO. A) Dependence of Ln ($[\mathrm{M}]_0/[\mathrm{M}]_t$) on the exposure time under NIR (red circles) and far-red (blue squares) irradiation. B) Dependence of Ln ($[\mathrm{M}]_0/[\mathrm{M}]_t$) on the exposure time under NIR (red circles) and far-red (blue squares) irradiation that was switched on and off. C) Dependence of M_n on the conversion under NIR and far-red irradiation. D) Molecular weight distributions after exposure to NIR irradiation for different periods of time.

Acknowledgements

We thank the University of New South Wales for funding and the Australian Research Council (ARC-FT).

Keywords: bacteriochlorophyll · controlled radical polymerization · photocatalysis · photoinduced electron transfer · RAFT polymerization

How to cite: *Angew. Chem. Int. Ed.* **2016**, *55*, 1036 – 1040
Angew. Chem. **2016**, *128*, 1048 – 1052

[1] R. E. Blankenship, H. Hartman, *Trends Biochem. Sci.* **1998**, *23*, 94 – 97.
[2] a) J. T. Beatty, J. Overmann, M. T. Lince, A. K. Manske, A. S. Lang, R. E. Blankenship, C. L. Van Dover, T. A. Martinson, F. G. Plumley, *Proc. Natl. Acad. Sci. USA* **2005**, *102*, 9306 – 9310; b) J. Xiong, W. M. Fischer, K. Inoue, M. Nakahara, C. E. Bauer, *Science* **2000**, *289*, 1724 – 1730.
[3] E. G. Nisbet, N. H. Sleep, *Nature* **2001**, *409*, 1083 – 1091.
[4] S. Molloy, *Nat. Rev. Microbiol.* **2005**, *3*, 582 – 582.
[5] a) G. Moad, E. Rizzardo, S. H. Thang, *Polymer* **2008**, *49*, 1079 – 1131; b) K. Matyjaszewski, N. V. Tsarevsky, *J. Am. Chem. Soc.* **2014**, *136*, 6513 – 6533; c) M. R. Hill, R. N. Carmean, B. S. Sumerlin, *Macromolecules* **2015**, *48*, 5459 – 5469.
[6] a) X. Pan, M. Lamson, J. Yan, K. Matyjaszewski, *ACS Macro Lett.* **2015**, *4*, 192 – 196; b) D. Konkolewicz, K. Schröder, J. Buback, S. Bernhard, K. Matyjaszewski, *ACS Macro Lett.* **2012**, *1*, 1219 – 1223; c) M. Chen, J. A. Johnson, *Chem. Commun.* **2015**, *51*, 6742 – 6745; d) F. Nzulu, S. Telitel, F. Stoffelbach, B. Graff, F. Morlet-Savary, J. Lalevee, L. Fensterbank, J.-P. Goddard, C. Ollivier, *Polym. Chem.* **2015**, *6*, 4605 – 4611; e) M. Ciftci, M. A. Tasdelen, Y. Yagci, *Polym. Chem.* **2014**, *5*, 600 – 606; f) E. Frick, A. Anastasaki, D. M. Haddleton, C. Barner-Kowollik, *J. Am. Chem. Soc.* **2015**, *137*, 6889 – 6896; g) M. Chen, M. J. MacLeod, J. A. Johnson, *ACS Macro Lett.* **2015**, *4*, 566 – 569; h) A. Ohtsuki, L. Lei, M. Tanishima, A. Goto, H. Kaji, *J. Am. Chem. Soc.* **2015**, *137*, 5610 – 5617; i) Q. Yang, F. Dumur, F. Morlet-Savary, J. Poly, J. Lalevée, *Macromolecules* **2015**, *48*, 1972 – 1980; j) Y. Yagci, M. A. Tasdelen, B. Kiskan, M. Çiftci, S. Dadashi-Silab, O. Suat Taskin, and G. Yilmaz in *Controlled Radical Polymerization*: *Mechanisms*, *Vol. 1187*, American Chemical Society, Washington, DC, **2015**, pp. 145 – 158; k) A. Ohtsuki, A. Goto, H. Kaji, *Macromolecules* **2013**, *46*, 96 – 102; l) A. Anastasaki, V. Nikolaou, F. Brandford-Adams, G. Nurumbetov, Q. Zhang, G. J. Clarkson, D. J. Fox, P. Wilson, K. Kempe, D. M. Haddleton, *Chem. Commun.* **2015**, *51*, 5626 – 5629; m) J. F. Quinn, L. Barner, C. Barner-Kowollik, E. Rizzardo, T. P. Davis, *Macromolecules* **2002**, *35*, 7620 – 7627; n) A. Anastasaki, V. Nikolaou, Q. Zhang, J. Burns, S. R. Samanta, C. Waldron, A. J. Haddleton, R. McHale, D. Fox, V. Percec, P. Wilson, D. M. Haddleton, *J. Am. Chem. Soc.* **2014**, *136*, 1141 – 1149; o) K. Koumura, K. Satoh, M. Kamigaito, *Polym. J.* **2009**, *41*, 595 – 603; p) K. Koumura, K. Satoh, M. Kamigaito, *Macromolecules* **2008**, *41*, 7359 – 7367; q) Y. Zhao, M. Yu, X. Fu, *Chem. Commun.* **2013**, *49*, 5186 – 5188; r) Y. Zhao, M. Yu, S. Zhang, Y. Liu, X. Fu, *Macromolecules* **2014**, *47*, 6238 – 6245; s) A. Fu, K. Gwon, M. Kim, G. Tae, J. A. Kornfield, *Biomacromolecules* **2015**, *16*, 497 – 506; t) Y. Shi, G. Liu, H. Gao, L. Lu, Y. Cai, *Macromolecules* **2009**, *42*, 3917 – 3926; u) G. Liu, H. Shi, Y. Cui, J. Tong, Y. Zhao, D. Wang, Y. Cai, *Polym. Chem.* **2013**, *4*, 1176 – 1182; v) Y. Shi, H. Gao, L. Lu, Y. Cai, *Chem. Commun.* **2009**, 1368 – 1370; w) T. G. Ribelli, D. Konkolewicz, S. Bernhard, K. Matyjaszewski, *J. Am. Chem. Soc.* **2014**, *136*, 13303 – 13312; x) M. Ciftci, M. A. Tasdelen, W. Li, K. Matyjaszewski, Y. Yagci, *Macromolecules* **2013**, *46*, 9537 – 9543; y) Y. Nakamura, T. Arima, S. Tomita, S. Yamago, *J. Am. Chem. Soc.* **2012**, *134*, 5536 – 5539; z) M. Tanabe, G. W. M. Vandermeulen, W. Y. Chan, P. W. Cyr, L. Vanderark, D. A. Rider, I. Manners, *Nat. Mater.* **2006**, *5*, 467 – 470; aa) X. Zheng, M. Yue, P. Yang, Q. Li, W. Yang, *Polym. Chem.* **2012**, *3*, 1982 – 1986; ab) E. Yoshida, *Colloid Polym. Sci.* **2010**, *288*, 73 – 78; ac) G. Zhang, I. Y. Song, K. H. Ahn, T. Park, W. Choi, *Macromolecules* **2011**, *44*, 7594 – 7599.
[7] H. Wang, Q. Li, J. Dai, F. Du, H. Zheng, R. Bai, *Macromolecules* **2013**, *46*, 2576 – 2582.
[8] a) K. D. Belfield, X. Ren, E. W. Van Stryland, D. J. Hagan, V. Dubikovsky, E. J. Miesak, *J. Am. Chem. Soc.* **2000**, *122*, 1217 – 1218; b) P. Xiao, F. Dumur, B. Graff, D. Gigmes, J. P. Fouassier, J. Lalevée, *Macromol. Rapid Commun.* **2013**, *34*, 1452 – 1458; c) M.-A. Tehfe, F. Dumur, B. Graff, D. Gigmes, J.-P. Fouassier, J. Lalevée, *Macromolecules* **2013**, *46*, 3332 – 3341; d) J. Vandenbergh, G. Reekmans, P. Adriaensens, T. Junkers, *Chem. Sci.* **2015**, *6*, 5753 – 5761; e) P. Xiao, F. Dumur, T. T. Bui, F. Goubard, B. Graff, F. Morlet-Savary, J. P. Fouassier, D. Gigmes, J. Lalevée, *ACS Macro Lett.* **2013**, *2*, 736 – 740; f) P. Xiao, J. Zhang, F. Dumur, M. A. Tehfe, F. Morlet-Savary, B. Graff, D. Gigmes, J. P. Fouassier, J. Lalevée, *Prog. Polym. Sci.* **2015**, *41*, 32 – 66; g) S. Telitel, F. Dumur, S. Telitel, O. Soppera, M. Lepeltier, Y. Guillaneuf, J. Poly, F. Morlet-Savary, P. Fioux, J.-P. Fouassier, D. Gigmes, J. Lalevee, *Polym. Chem.* **2015**, *6*, 613 – 624; h) J. Morris, S. Telitel, K. E. Fairfull-Smith, S. E. Bottle, J. Lalevee, J.-L. Clement, Y. Guillaneuf, D. Gigmes, *Polym. Chem.* **2015**, *6*, 754 – 763; i) X. Wang, G. Liu, J. Hu, G. Zhang, S. Liu, *Angew. Chem. Int. Ed.* **2014**, *53*, 3138 – 3142; *Angew. Chem.* **2014**, *126*, 3202 – 3206.
[9] a) B. P. Fors, C. J. Hawker, *Angew. Chem. Int. Ed.* **2012**, *51*, 8850 – 8853; *Angew. Chem.* **2012**, *124*, 8980 – 8983; b) J. E. Poelma, B. P. Fors, G. F. Meyers, J. W. Kramer, C. J. Hawker, *Angew. Chem. Int. Ed.* **2013**, *52*, 6844 – 6848; *Angew. Chem.* **2013**, *125*, 6982 – 6986.
[10] K. Schröder, K. Matyjaszewski, K. J. T. Noonan, R. T. Mathers, *Green Chem.* **2014**, *16*, 1673 – 1686.
[11] J. Xu, K. Jung, A. Atme, S. Shanmugam, C. Boyer, *J. Am. Chem. Soc.* **2014**, *136*, 5508 – 5519.
[12] S.-i. Sasaki, H. Tamiaki, *J. Org. Chem.* **2006**, *71*, 2648 – 2654.
[13] C. Musewald, G. Hartwich, F. Pöllinger-Dammer, H. Lossau, H. Scheer, M. E. Michel-Beyerle, *J. Phys. Chem. B* **1998**, *102*, 8336 – 8342.
[14] T. M. Cotton, R. P. Van Duyne, *J. Am. Chem. Soc.* **1979**, *101*, 7605 – 7612.
[15] a) L. Lu, N. Yang, Y. Cai, *Chem. Commun.* **2005**, 5287 – 5288; b) J. Xu, S. Shanmugam, N. A. Corrigan, C. Boyer in *Controlled Radical Polymerization*: *Mechanisms*, *Vol. 1187*, American Chemical Society, Washington, DC, **2015**, pp. 247 – 267, Chapter 13, DOI: 10.1021/bk-2015-1187.ch013; c) M. A. Tasdelen, Y. Y. Durmaz, B. Karagoz, N. Bicak, Y. Yagci, *J. Polym. Sci. Part A* **2008**, *46*, 3387 – 3395; d) L. Lu, H. Zhang, N. Yang, Y. Cai, *Macromolecules* **2006**, *39*, 3770 – 3776.
[16] a) S. Shanmugam, C. Boyer, *J. Am. Chem. Soc.* **2015**, *137*, 9988 – 9999; b) S. Shanmugam, J. Xu, C. Boyer, *J. Am. Chem. Soc.* **2015**, *137*, 9174 – 9185; c) J. Xu, K. Jung, C. Boyer, *Macromolecules* **2014**, *47*, 4217 – 4229; d) S. Shanmugam, J. Xu, C. Boyer, *Chem. Sci.* **2015**, *6*, 1341 – 1349; e) J. Xu, S. Shanmugam, C. Boyer, *ACS Macro Lett.* **2015**, *4*, 926 – 932.
[17] a) N. Tessler, V. Medvedev, M. Kazes, S. Kan, U. Banin, *Science* **2002**, *295*, 1506 – 1508; b) L. R. Hirsch, R. J. Stafford, J. A. Bankson, S. R. Sershen, B. Rivera, R. E. Price, J. D. Hazle, N. J. Halas, J. L. West, *Proc. Natl. Acad. Sci. USA* **2003**, *100*, 13549 – 13554; c) R. Aswathy, Y. Yoshida, T. Maekawa, D. S. Kumar, *Anal. Bioanal. Chem.* **2010**, *397*, 1417 – 1435; d) M. S. Yavuz, Y. Cheng, J. Chen, C. M. Cobley, Q. Zhang, M. Rycenga, J. Xie, C. Kim, K. H. Song, A. G. Schwartz, L. V. Wang, Y. Xia, *Nat. Mater.* **2009**, *8*, 935 – 939.

Received: October 28, 2015
Published online: December 3, 2015

